LA-5434-MS

INFORMAL REPORT

Scaling Laws for the Linear Theta Pinch: A Comparison of Magnetic and Laser Heating

los alamos scientific laboratory

of the University of California

LOS ALAMOS, NEW MEXICO 87544

UNITED STATES
ATOMIC ENERGY COMMISSION
CONTRACT W-7405-ENG. 36

In the interest of prompt distribution, this LAMS report was not edited by the Technical Information staff.

Printed in the United States of America. Available from
National Technical Information Service
U. S. Department of Commerce
5285 Port Royal Road
Springfield, Virginia 22151
Price: Printed Copy $4.00; Microfiche $1.45

LA-5434-MS
Informal Report
UC-20
ISSUED: October 1973

los alamos
scientific laboratory
of the University of California
LOS ALAMOS, NEW MEXICO 87544

Scaling Laws for the Linear Theta Pinch: A Comparison of Magnetic and Laser Heating

by

W. R. Ellis
G. A. Sawyer

SCALING LAWS FOR THE LINEAR THETA PINCH, I:

A COMPARISON OF MAGNETIC AND LASER HEATING

TABLE OF CONTENTS

PAGE

SCALING LAWS FOR THE LINEAR THETA PINCH, I:
A COMPARISON OF MAGNETIC AND LASER HEATING

by

W. R. Ellis and G. A. Sawyer

ABSTRACT

The scaling laws for a linear theta-pinch reactor are developed. Conventional magnetic heating and laser heating of the plasma are compared. It is shown that, if a confining magnetic field of 400 kG is used, a power producing reactor need be only 1.2 km long.

I. INTRODUCTION

Recent interest has been expressed by Dawson, Hertzberg, Vlases,[1,2,3] and others in the proposal to heat a long, dense plasma column with a CO_2 laser beam. This type of heating has been proposed in conjunction with large axial magnetic fields of the type found in conventional linear θ-pinches, but of substantially higher field strength - up to one megagauss in some cases. The present report examines the feasibility and necessity of such high fields, and compares the performance of the high field, laser-heated pinch with that of a conventional, magnetically heated θ-pinch operated at the same field strength.

It is well-known that operation at higher field strengths reduces the length requirements for a linear reactor. Operation at megagauss field strengths, as has been optimistically proposed by some proponents of the laser-heating method, reduces the length requirements of a reactor to around 200 meters for an $n\tau$ of 10^{15} cm^{-3} sec. Such a proposal is obviously attractive, but appears to be a practical impossibility on the basis of present day high-field technology.

We undertake to derive some basic scaling relationships which will apply to either of these reactor concepts. The scaling laws are based upon idealized reactor and plasma physics models and emphasize basic physics as opposed to engineering. We assume throughout that the length of a linear reactor is determined by particle end loss rather than by axial electron thermal conduction. Radial diffusion and heat transport are assumed small compared to axial losses. In order to avoid specific designs for the compression coil and blanket, an overall energy balance for the reactor systems has not been attempted. However, scaling laws for the thermal output power and magnetic energy storage requirements have been derived, based on a compression coil located inside the blanket.

In order to minimize the length (and hence cost) of the power plant, a theta-pinch reactor should operate at the highest possible plasma density, and therefore, for a given temperature, at the highest possible magnetic field. We find that 300-500 kG fields are experimentally obtainable, and that a reactor can probably be as short as 1 km with only self-mirroring to reduce the end loss. We select operation at 400 kG as a reasonable design point for the high-density theta pinch in the present study.

For a conventional magnetically heated θ-pinch operated at 400 kG we arrive at the following set of self-consistent reactor parameters: a coil radius b of $\sim$ 2 cm, a plasma radius a of 0.15 cm, a plasma density n of 2 x 10^{17}, a minimum length L = 1.2 km, and a stored magnetic energy E_M of $\sim$ 1 GJ.

For a laser-heated θ pinch, we find that laser absorption length considerations impose a length requirement which is easily compatible with the length required by end loss considerations. In order to keep the required laser energy reasonably low, it is necessary to keep the plasma radius small, a few mm. We conclude that a laser-heated reactor might have parameters B = 400 kG, b = 1.0 cm, a = 0.1 cm, $n = 2 \times 10^{17}$, L = 1.2 km, E_M = 250 MJ, and laser output energy E_L = 5 MJ.

From this preliminary study, we are unable to reach any persuasive conclusions regarding the desirability of laser-heating over conventional theta-pinch heating, or vice versa. Rather, they appear to us at this time to be alternative methods whose relative merits require further study. The best system may well involve some features of both, such as laser preheat followed by adiabatic magnetic compression. In such a hybrid system, the laser heating would replace the shock-heating stage of a conventional θ-pinch.

We note, finally, that the high density linear θ-pinch as modeled here has some inherent advantages over conventional toroidal designs from a reactor point of view. These include easy access from the ends, a much smaller minimum plant size, and more efficient use of the magnetic field.

The laser method, of course, does not lend itself readily to a toroidal design.

II. MAGNETIC PRESSURE CONSIDERATIONS

A. Plasma Pressure Balance

A plasma confined in equilibrium in a magnetic field has a density proportional to $\beta B^2/T$, assuming equal electron and ion temperatures:

$$n = 1.24 \times 10^{13} \frac{\beta B^2(\mathrm{kG})}{kT(\mathrm{keV})} \ \mathrm{cm}^{-3} \quad . \qquad (1)$$

For plasmas of thermonuclear interest, kT is limited to the approximate range $5 \leq kT \leq 15$ keV, and for our calculations we will assume $\overline{kT}$ = 10 keV during the "burn". Eq. (1) is plotted in Fig. 1 for the case β = 1. We see that for "typical" θ-pinch reactor parameters,[4] $\overline{kT}$ = 10 keV, B = 150 kG, the ion density which can be contained is ∿ 2.8 $\times 10^{16}$ cm^{-3}. In order to operate at higher densities, the magnetic field strength must increase quadratically in proportion. At 10^{18} cm^{-3}, for example, the required magnetic field strength is about 900 kG.

B. Strength of Materials

The maximum magnetic field that can be used will be governed by strength of materials since the coil winding must be capable of supporting the magnetic pressure produced by the confinement field, whether dc or pulsed.

1. Pulsed Fields. For pulsed fields produced by single turn solenoids as in theta pinches, the magnetic pressure must be supported by the first coil surface. Knoepfel[5] gives a complete discussion of pulsed field techniques. Figure 2 shows the magnetic pressure (in psi) which is associated with the magnetic field strength B (in kG). The pressure exerted by a one megagauss field is nearly 600,000 psi, which is above the yield strength of any presently known structural material. Maraging steel is capable of holding about 600 kG, and 7075 aluminum (of which the Scyllac coil is made), about 300 kG. The single-turn coils fail at the ends where flux is concentrated at the corners. Typical field strengths may be twice the axis field strength even with rounding of the corners. The highest field on axis achieved at LASL in single-turn-steel-mirror coils for Scyllac is about 250 kG.[6] A single-turn bubble chamber magnet has been reported to achieve 300 kG.[7] About 300 kG probably represents the state of the art in pulsed coils of several centimeter bore that survive many pulses. These field levels are accomplished in massive single-turn solenoids. Generally, other designs such as helix coils have not done as well.[8]

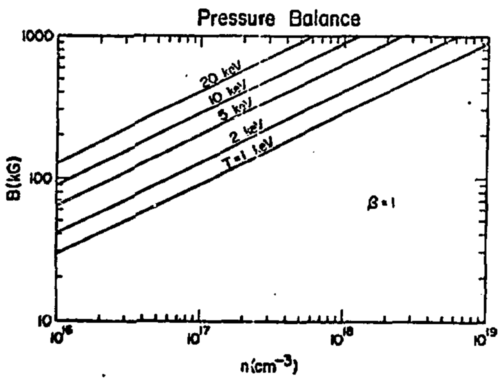

Fig. 1. Magnetic field required for pressure balance.

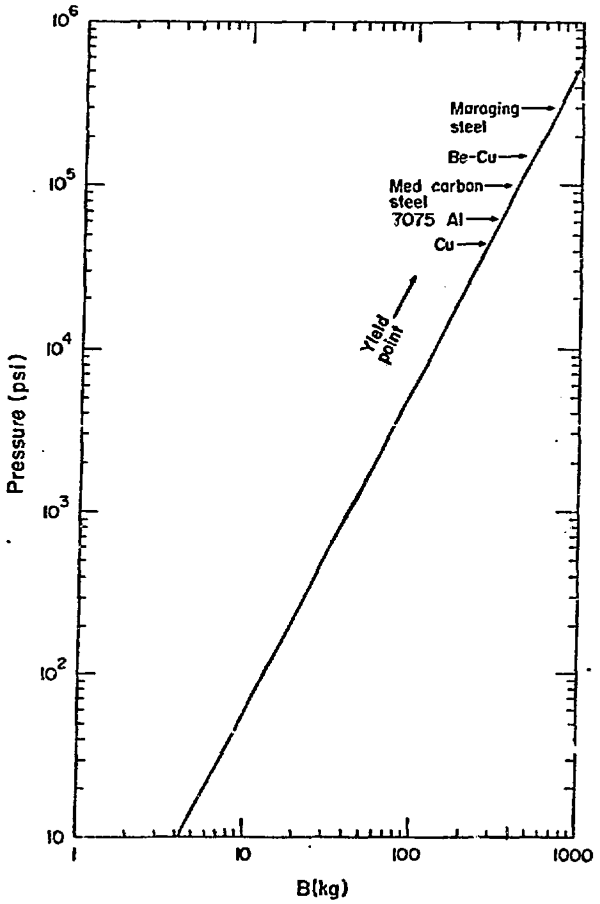

Fig. 2. Magnetic pressure vs B.

Knoepfel and Lupi have recently written an excellent review article on pulsed fields[9] in which they report achieving 650 kG in a 1 cm bore coil. This coil represents the present state of the art for coils which survive many pulses and have a field volume of more than 1 cm^3. It was made of massive steel jaws which enclosed a shaped tantalum insert to concentrate the flux. The impact strength or toughness of tantalum and its high melting point are the properties that make it a desirable material for high-field solenoids. At 650 kG, the surface magnetic pressure exceeds the yield strength of tantalum by a factor four, but it yields only gradually to successive impacts and is able to survive more than 20 pulses. However, at 650 kG, the high melting point of tantalum is more important than its strength. Surface melting due to resistive heating of the surface is a major consideration at high fields. The critical magnetic field for melting depends on the current pulse shape, but is typically 500–700 kG for copper and 660–930 kG for tantalum.[9]

It is possible, in principle, to eliminate the problems of surface pressure and melting that are characteristic of single-turn solenoids by layering or litzing the coil. Some attempts have been made to make multilayer coils,[10] but the highest fields achieved are less than those for single-layer solenoids. Since such coils are necessarily complex, they will be subject to new strength and cost considerations. We suspect that practical field limits are not far different from those for single-layer solenoids.

Higher magnetic fields have been made, of course, but the methods are not suitable for CTR use. Fields up to about 900 kG have been reached in small coils (∿ 5 mm bore) of limited lifetime[10-13] and still higher fields, up to 10 MG, have been achieved with high explosives.[5,14]

2. DC Fields. If DC fields or slowly varying pulse fields are produced, skin effect is not a factor and the first surface need not bear the total pressure. Strength, however, is not the limiting parameter. Power consumption and cooling problems are formidable at fields above about 200 kG, and the largest fields reported are about 250 kG.[9,15,16,17] Bruce Montgomery at the Francis Bitter National Magnet Laboratory has described plans for a hybrid conventional-superconducting magnet to operate at 250 kG in a 3-cm bore.[15] Its power consumption will be 6 MW.

Superconducting coils would eliminate the excessive power consumption of dc coils, but the best superconducting coils at present are made of Nb_3Sn, which has a critical field of 160 kG at 4.2 °K. A 150 kG superconductor magnet has been constructed.[17] A higher critical field of 410 kG exists for NbAlGe alloy[18] but magnets have not been fabricated.

3. Maximum Practical Magnetic Fields. The largest magnetic fields have been obtained in single-turn solenoids. The limits for coils that last many shots are about 600 kG for coils of 1 cm bore and 300 kG for coils of 10 cm bore. One MG is definately out of reach with present technology.

III. SCALING LAWS FOR THERMONUCLEAR POWER PRODUCTION IN A PULSED REACTOR.

The average thermal power output per unit length in a pulsed reactor is

$$\frac{P_{Th}}{L} = \frac{1}{\tau_c}\frac{E_n}{L} \quad , \tag{2}$$

where τ_c is the cycle time, i.e., the number of seconds between the start of successive burning pulses, and E_n/L is the energy release per unit length per burning pulse.

A. Rate of Energy Production

In a thermonuclear plasma containing deuterium (D) and tritium (T) ions, the reaction rate is given by

$$R = n_D\, n_T\, \overline{\sigma v} \quad \text{reactions/cm}^3\text{/sec} \tag{3}$$

where $\overline{\sigma v}$ is the Maxwell-averaged D-T cross-section and n_D and n_T are the density of deuterium and tritium, respectively. If we assume a 50-50 mixture of D-T ($n_D = n_T = n/2$) and assign an energy release of Q_n* per reaction, the rate of energy production per unit length of reactor becomes

$$\frac{P_n}{L} = \frac{\pi}{4}\, a^2\, n^2\, Q_n\, \overline{\sigma v} \quad . \tag{4}$$

In a "burning pulse" of duration τ_B the energy release is

$$\frac{E_n}{L} = \frac{\pi}{4}\, a^2\, n^2\, Q_n\, \overline{\sigma v}\, \tau_B \quad , \tag{5}$$

and the thermal power output, from Eq. (2), is

$$\frac{P_{Th}}{L} = \frac{\pi}{4}\, a^2\, n^2\, Q_n \overline{\sigma v}\, \frac{\tau_B}{\tau_c} \quad . \tag{6}$$

Equation (5) for the energy released per unit length of reactor is worth some comments. Rearranging we have

$$\frac{E_n}{L} = a^2 n \times \left[\frac{\pi}{4}\ Q_n\, \overline{\sigma v}\, n\tau_B\right] \quad . \tag{7}$$

In most cases of interest the quantity $n\tau_B$ will have a well-defined value, e.g., $n\tau_B = 10^{15}$ cm^{-3} sec for a net power-producing reactor. The temperature in a reactor will also have a well-defined value, e.g., $k\overline{T} = 10$ keV. Q_n is a constant by definition: $Q_n =$ 18.9 MeV = 3.03×10^{-12} joules. Thus the quantity in brackets is constant for a given reactor, i.e.,

$$\frac{E_n}{L} = a^2 n \times \text{constant} \quad . \tag{8}$$

Furthermore, since the units of $n\tau_B$ are cm^{-3} sec and the units of $\overline{\sigma v}$ are cm^3 sec^{-1}, the product $n\tau_B\, \overline{\sigma v}$ is a dimensionless constant. For $n\tau_B = 10^{15}$ cm^{-3} sec and $k\overline{T} = 10$ keV ($\overline{\sigma v} = 1.1 \times 10^{-16}$ cm^3 sec^{-1}), $n\tau_B\, \overline{\sigma v} = 0.11$. Thus the constant in Eq. (8) has the units of Q_n, or energy; in convenient units,

$$\frac{E_n}{L}\left(\frac{\text{MJ}}{\text{m}}\right) = a^2(\text{cm})\ n(\text{cm}^{-3}) \times \left[2.6 \times 10^{-17}\right]. \tag{9}$$

The quantity a^2n in Eq. (7) is simply the line density, or total particles per unit length, which is proportional to the filling pressure, other things being equal. That is, the output power of a pulsed reactor,

$$\frac{P_{Th}}{L}\ (\text{MW}) = \frac{a^2(\text{cm})\ n(\text{cm}^{-3})}{\tau_c(\text{sec})} \times \left[2.6 \times 10^{-17}\right] \tag{10}$$

is directly proportional to the filling pressure, and the burning time, τ_B, decreases inversely with the compressed density achieved.

Finally, from the pressure balance condition, Eq. (1), we can replace n by B^2:

$$\frac{E_n}{L} = a^2B^2 \times \text{constant}$$

$$= a^2(\text{cm})\ B^2(\text{kG}) \times \left[3.22 \times 10^{-5}\right]\ \frac{\text{MJ}}{\text{m}} \ . \tag{11}$$

B. First Wall Loading and Maximum Cycle Rate

In a pulsed reactor the cycle time τ_c is an adjustable parameter which can be used to limit the neutron load at the first wall resulting from

*Here we take Q_n = 14.1 MeV birth energy per neutron, plus 4.8 MeV from the Li^6 (n,α) T breeding reaction in the blanket. The 3.52 MeV birth energy of the confined alpha particles is not counted in Q_n. The quantity P_n refers to the energy release associated with neutrons.

uncollided (14.06 MeV) neutrons to 3.5 MW/m^2 (350 watts/cm^2) or less.[4] The wall loading, $\overline{P}_w/A$, is

$$\overline{P}_w/A = \frac{E_n}{L} \; \frac{14.06}{Q_n} \; \frac{1}{2\pi b \tau_c} \tag{12}$$

$$= \frac{E_n}{L}\left(\frac{MJ}{m}\right) \times \frac{0.118}{b(m)\ \tau_c(sec)} \ \frac{MW}{m^2} \ .$$

Thus, for a fixed output energy per unit length of reactor per pulse, E_n/L = constant, $\overline{P}_w/A$ can be controlled by varying either b or τ_c. However, for a fixed output power per unit length, $E_n/L\tau_c$ = constant, $\overline{P}_w/A$ can only be adjusted by varying b. If we removed these restrictions on energy and power, then $\overline{P}_w/A$ scales as, from Eqs. (9) and (12),

$$\overline{P}_w/A = \frac{a^2 n}{b\tau_c} \quad \times \quad \text{constant} \tag{13a}$$

$$= \frac{a^2(cm)\ n(cm^{-3})}{b(cm)\ \tau_c(sec)} \times \left[3.07 \times 10^{-16}\right] \frac{MW}{m^2}$$

or, in terms of B, using (1),

$$\overline{P}_w/A = \frac{a^2\ B^2}{b\ \tau_c} \times \text{const.} \tag{13b}$$

$$= \frac{a^2(cm)\ B^2(kG)}{b(cm)\ \tau_c(sec)} \times \left[3.80 \times 10^{-4}\right] \frac{MW}{m^2} .$$

Finally we calculate the thermal power output per unit length of the reactor, from Eq. (2) and (12):

$$\frac{P_{Th}}{L} = 8.47 \times 10^{-2}\ b(cm)\ \overline{P}_w/A \left(\frac{MW}{m^2}\right) \quad \frac{MW}{m} \cdot \tag{14}$$

Note that the thermal power output per unit length is independent of all plasma properties, and is determined only by the coil radius and acceptable wall loading. It is also independent of the magnetic field.

IV. SCALING LAWS FOR THE LINEAR θ-PINCH

Scaling laws for the linear θ-pinch are derived below in which the independent variable is taken to be the magnetic field strength, B.

A. Length of a θ-Pinch Reactor

If we assume a β = 1 plasma at an average temperature of 10 keV in the reactor during the burn [for example, kT equals 5 keV at the start of ignition and 15 keV at the finish, due to α particle heating], then the average density during the burn is given by, from (1),

$$\overline{n} = 1.24 \times 10^{12}\ B^2(kG) \quad cm^{-3} \quad . \tag{15}$$

1. Lawson Criterion. The Lawson criterion is taken to be, for a net power-producing reactor,

$$\overline{n}\tau_B = 10^{15}\ cm^{-3}\ sec \quad . \tag{16}$$

Eliminating $\overline{n}$ between (15) and (16) yields

$$\tau_B = \frac{806}{B^2} \ \ sec \tag{17}$$

for B in kG. In a recent RTPR design,[19] for example, B is 110 kG and τ_B is approximately 80 msec.

2. End Loss Time. We assume that confinement is limited by particle loss out of the open ends of the θ-pinch. If we define the end-loss rate in terms of an effective e-folding time,

$$\frac{dn}{dt} = -\frac{1}{\tau_{EL}}\ n \tag{18}$$

and assume the maximum loss rate for a Maxwellian distribution of velocities (i.e., a full loss-cone), then the loss time has been given by Freidberg[20] as

$$\tau_{EL} = \left(\frac{\pi}{2}\right)^{1/2}\left(\frac{m_i}{kT}\right)^{1/2} \frac{L}{\eta} \ , \tag{19}$$

where m_i is the mass of an "average" D-T ion,

$$m_i = \frac{m_D + m_T}{2} = 4.2 \times 10^{-24}\ \text{grams}, \tag{20}$$

L is the total length of the θ-pinch, and

$$\eta = \frac{1 + \sqrt{1-\beta}}{2\ R_{applied}} \tag{21}$$

is a "mirror" parameter which includes both applied-mirror and self-mirroring effects. $R_{applied}$ = 1 for no applied mirrors, in which case η = 1/2 and

$$\tau_{EL}(sec) = 4.1 \times 10^{-6}\ L(m) \quad . \tag{22}$$

For an applied mirror ratio of 4, τ_{EL} (sec) ≈ 10^{-6} L(m), etc. For the remainder of this report, we will assume only self-mirroring, R = 1.

Taylor and Wesson[21] have also treated the problem of end loss from a θ-pinch, taking as their model a steady, ideal MHD flow through a magnetic orifice. Their model predicts a self-mirroring (R = 1) end loss time of

$$(\tau_{EL})_{T-W} = \left(\frac{1}{\gamma}\right)^{1/2} \left(\frac{m_i}{kT}\right)^{1/2} \frac{L}{\eta_{T-W}} \qquad (19a)$$

where γ is the ratio of specific heats, taken here as 5/3, and the mirror parameter is

$$\eta_{T-W} = 2\sqrt{1-\beta} \quad . \qquad (21a)$$

The Taylor-Wesson model predicts the unrealistic result of zero end-loss for β = 1 (i.e., perfect self-mirroring) and agrees numerically with the Freidberg formula for β = 0.97. In view of these facts, the Taylor-Wesson model is poorly suited to our β ≈ 1 assumption, and will not be used.

Recent experiments[22] on a 5 meter linear θ-pinch at LASL give times shorter than Eq. (19) by a factor of 2 to 3, but confirm the scaling with L and kT.

For the purposes of this report we will use the uncorrected Freidberg formula, Eq. (22). This assumption is justified because of (a) a lack of experimental data in long, collisionless θ-pinches, and (b) the likelihood that some form of end-stoppering (effective R > 1) will be applied.

3. End-Loss Length. An estimate of the machine length L can be obtained by equating the burn time from the Lawson criterion, Eq. (17), to the end loss time, Eq. (22). Thus

$$L = \frac{1.97 \times 10^8}{B^2(\text{kG})} \text{ meters,} \qquad (23)$$

or in terms of the density,

$$L = \frac{2.44 \times 10^{20}}{\bar{n}(\text{cm}^{-3})} \text{ meters} \quad . \qquad (24)$$

Equations (23) and (24) are plotted in Figs. (3) and (4) as the curves for $\bar{n}\tau = 10^{15}$ cm^{-3} sec. Also shown are curves for $\bar{n}\tau = 10^{14}$, which is the appropriate $\bar{n}\tau$ value for a scientific feasibility

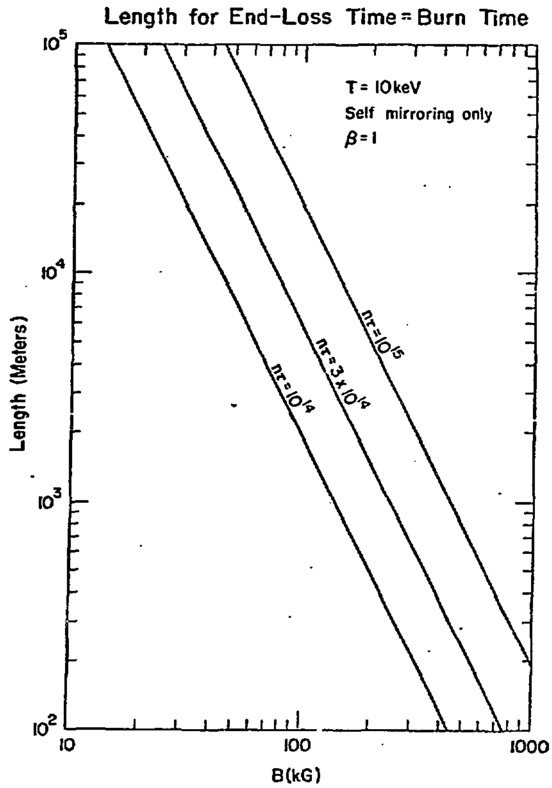

Fig. 3. Minimum reactor length vs magnetic field [Plot of Eq. (23)].

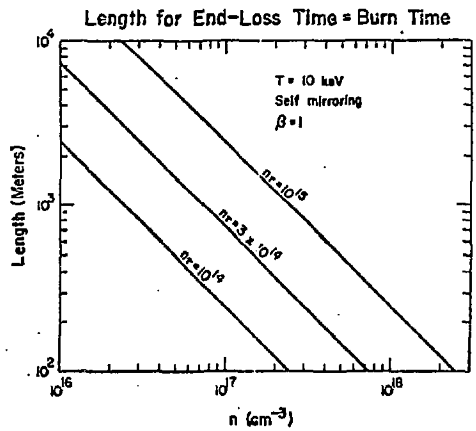

Fig. 4. Minimum reactor length vs ion density [Plot of Eq. (24)].

experiment. Increasing B from 100 kG to 500 kG will reduce the length of a θ-pinch reactor from 19.7 km (12.2 miles) to 788 meters (.49 miles), which is equivalent to a reduction in capital cost for the reactor of about a factor of 25 - a very desirable result.

B. Optimum Coil Bore.

The optimum length for a θ-pinch reactor is clearly the minimum length, but the optimum bore is not so easily defined. In the discussion below we examine the optimum bore, $b_{opt}(B)$, which results from considering 4 different conceptual models of the plasma heating. We conclude that a reasonable choice is $b_{opt} \simeq 2$ cm, independent of B. This conclusion leads to a magnetic energy storage requirement for the reactor which is also independent of B, as discussed in Sec. IV-D.

1. Model 1: Staged θ-Pinch with Adiabatic Compression and Fast Implosion Heating.

(a). Choice of Compression Ratio. In the staged θ-pinch concept,[4] plasma heating is accomplished by a combination of shock (or implosion) heating and subsequent adiabatic compression in a rising magnetic field. The minimum coil bore of such a device is determined by the compression ratio X_o = a/b (b is the coil radius) and the minimum radius a to which the plasma can be compressed.

In the toroidal θ-pinch design,[4] a balance must be struck between wall stabilization considerations on the one hand, which require "fat" plasmas (large a/b ratio), and practical limits to E_θ on the other hand, which require "skinny" plasmas (small a/b ratio). In the linear θ-pinch concept, the plasma is theoretically MHD stable. There is no need for wall stabilization, and the conflict which arises in the toroidal case disappears. In the linear θ-pinch, therefore, we anticipate the use of large compression ratios and a large amount of compressional heating.

We will assume throughout that the ignition temperature is 5 keV, and that the plasma beta is unity at ignition.

For a programmed implosion (the so-called "free-expansion" model) where the equilibrium radius after the implosion (before adiabatic compression is a = 0.76b, ($X_s \simeq 0.76$), the final temperature reached after compression is related to the applied electric field, E_θ, by [4,19]

$$E_\theta\left(\frac{kV}{cm}\right) = 0.244\ X_o^{7/3}\ [kT(keV)]^{1/2}\ B(kG). \qquad (25)$$

For kT = 5 keV, and the same units,

$$E_\theta = 0.546\ X_o^{7/3}\ B\ . \qquad (26)$$

Since applied E_θ's in the several kV/cm range are technologically difficult to achieve, we will limit consideration here to $E_\theta \simeq 1$ kV/cm and rely on adiabatic compression for the remainder of the heating. In this case (26) becomes

$$X_o \simeq \frac{1.30}{B^{3/7}\ (kG)}\ . \qquad (27)$$

(b). Minimum Plasma Radius. We will estimate the minimum plasma radius in two ways: 1) by assuming that the plasma in compression has a radius given by the "sheath width" c/ω_{pi};[23] and 2) by assuming that the plasma radius is limited to an ion gyroradius. The two methods are easily shown to be equivalent, and for β = 1, they give the same answer. For brevity, we will only develop the gyroradius model here.

The gyroradius, r_B, for a particle of charge q, mass m, and velocity v is, in MKS units,

$$r_B \simeq \frac{mv}{qB}\ . \qquad (28)$$

Since there are two degrees of freedom perpendicular to the magnetic field lines, the energy of gyration, $1/2\ mv^2$, is equal to kT for a Maxwellian distribution, giving

$$r_B \simeq \frac{\sqrt{2mkT}}{qB}\ . \quad \text{(MKS)} \qquad (29)$$

Neglecting alpha particles (which, for early times, do not exist), the largest gyroradius in the plasma is, from (29), associated with tritons. At 5 keV the triton gyroradius is

$$r_B(T) = \frac{16.2}{B(kG)}\ \text{cm}\ . \qquad (30)$$

Now assuming that a $\simeq r_B$(T) yields, from (30),

$$X_o = \frac{16.2}{b(\text{cm})\ B(\text{kG})} = \frac{a}{b} \quad , \tag{31}$$

and from Eqs.(31) and (27),

$$b_{min} = \frac{12.5}{B^{4/7}\ (\text{kG})}\ \text{cm} \quad , \tag{32}$$

as the minimum coil radius consistent with heating to 5 keV.

At 100 kG, 300 kG, and 500 kG, b_{min} is 0.90 cm, 0.48 cm, and 0.36 cm respectively. These coil radii are small compared to conventional θ-pinch machines, and while advantageous from the viewpoint of making large fields, would probably not permit efficient implosion heating, since the sheath width during implosion, ($c/\omega_{pi} \sim 1$ cm), would exceed the coil radius b_{min}.

2. Model 2: Adiabatic Compression Alone. The linear θ-pinch is capable, in principle, of reaching its ignition temperature of 5 keV by adiabatic compression alone. If we take the starting radius for compression as b, and assume a typical preionization temperature of 2 eV for the starting temperature T_1, then from the adiabatic law (assuming 3 degrees of freedom, i.e., $\gamma = 5/3$):

$$\frac{T_1}{T_2} = \left(\frac{a}{b}\right)^{4/3} \quad . \tag{33}$$

Using Eq. (31) for a/b, we have

$$b_{min} = \frac{5728}{B(\text{kG})}\ \text{cm} \ . \tag{34}$$

At 100 kG, 300 kG, and 500 kG, b_{min} is 57 cm, 19 cm, and 11 cm, respectively. These radii are so large that the magnetic energy storage requirements would be prohibitive. In addition, operation at high fields would be ruled out by strength-of-materials considerations. These facts suggest that some form of preheating is practically unavoidable in a θ-pinch, prior to adiabatic compression.

3. Model 3: Include Self-Consistent E_θ for Adiabatic Compression. A certain amount of E_θ is automatically provided in a θ-pinch, according to Faraday's law:

$$\nabla \times \overline{E} = - \frac{\partial \overline{B}}{\partial t}\ (\text{MKS}) \ . \tag{35}$$

In convenient units this self-consistent field is given by

$$E_\theta \left(\frac{\text{kV}}{\text{cm}}\right) = \frac{10^{-8}}{2} \quad \frac{b(\text{cm})\ B(\text{kG})}{\tau_R} \tag{36}$$

where τ_R is the risetime of the B field in seconds.

If we express the risetime of the field as the fraction α of the burn time, $\tau_R/\tau_B = \alpha$, then from Eq. (17)

$$\tau_R = \frac{806\ \alpha}{B^2(\text{kG})}\ \text{sec} \ . \tag{37}$$

Combining Eqs.(36) and (37) yields the self-consistent electric field:

$$E_\theta \left(\frac{\text{kV}}{\text{cm}}\right) = \frac{10^{-8}}{1612\ \alpha}\ b\ B^3 \quad . \tag{38}$$

The appropriate value of X_s for a linearly rising B field ($\tau_R >>$ implosion time) has been estimated by Ribe[24] as $X_s = 0.3$. In this case the coefficient in Eq. (25) must be increased by a factor proportional to $X_s^{10/3}$, i.e., $(0.76/0.3)^{10/3} = 22.2$. Thus

$$E_\theta \left(\frac{\text{kV}}{\text{cm}}\right) = 5.4\ X_o^{7/3}\ [kT(\text{keV})]^{1/2}\ B(\text{kG}). \tag{39}$$

Eliminating E_θ between Eqs.(38) and (39) yields the compression factor (for 5 keV):

$$X_o = \left(2.57 \times 10^{-12}\ \frac{b\ B^2}{\alpha}\right)^{3/7} . \tag{40}$$

Finally, eliminating X_o between Eqs.(31) and (40) yields the self-consistent solution for b_{min}:

$$b_{min} = \frac{2.11 \times 10^4\ \alpha^{3/10}}{B^{13/10}\ (\text{kG})}\ \text{cm} \quad . \tag{41}$$

Thus, for example, if $\alpha = 0.1$ ($\tau_R = \tau_B/10$), for B = 100 kG, 300 kG, and 500 kG, we find b_{min} = 27 cm, 6.4 cm, and 3.3 cm, respectively. These values for b are better than Model 2, where E_θ was neglected, but not competitive with Model 1, where E_θ was applied by separately-energized shock circuits. This is because the self-consistent E_θ field will be smaller than any reasonable value of the applied E_θ field by the ratio of rise times. In the 300 kG case above, for example, $\tau_B = 806/B^2 = 8.96$ msec, $\tau_R = \tau_B/10 = 0.896$ msec, and E_θ = 11 V/cm. The conclusion is that the self-consistent E_θ doesn't help much.

4. Model 4: Legislate b = Constant. In many respects, the most satisfactory scaling law for b(B) is perhaps the most obvious - namely, legislating b = constant, independent of the magnetic field.

If conventional implosion heating is used in a device with a fixed bore of, say, b = 2 cm, then the calculations given above for Model 1 show that the plasma can be heated to ignition while at the same time being somewhat "under-compressed." This would produce a reactor plasma similar to the plasmas being studied in the Los Alamos Scylla series of experiments ($a \sim 3\text{-}4\ r_B$).

From Eq. (26) the compression ratio is given by

$$X_o = \frac{a}{b} = \left[1.83\ \frac{E_\theta\ (\text{kV/cm})}{B(\text{kG})}\right]^{3/7} . \qquad (42)$$

For b = 2 cm, the plasma radius after compression is

$$a = 2.59\ \frac{E_\theta^{3/7}\ (\text{kV/cm})}{B^{3/7}\ (\text{kG})}\ \text{cm} . \qquad (43)$$

For a rather modest applied electric field of, say, E_θ = 500 V/cm, the radius a(B) is given by

$$a = \frac{1.92}{B^{3/7}\ (\text{kG})}\ \text{cm} . \qquad (44)$$

For B = 100, 300, and 500 kG, we find a = 0.27 cm, 0.17 cm, and 0.13 cm, respectively. These numbers correspond to a few gyroradii in each case, which is probably more realistic than assuming a = one gyroradius. For the remainder of this paper we will use the scaling results given in Model 4, and assume that b = 2 cm, independent of B.

C. Alpha Particle Plasma Sheaths.

As the thermonuclear burn progresses, alpha particles are produced in the plasma with a birth energy of 3.52 MeV. These particles will be confined by the magnetic field and at the end of the burn the plasma will contain ∿ 5% alpha particles. At 3.52 MeV, the alpha particle gyroradius is given by

$$r_B(\alpha) = \frac{272}{B}\ \frac{\text{cm}}{(\text{kG})} . \qquad (45)$$

In order to avoid alpha particle collisions with the coil wall, the alpha particle gyroradius $r_B(\alpha)$, should be kept smaller than b. This requires operation at field strengths above 137 kG for b = 2 cm.

The question of the development of alpha particle sheaths during the burn is an important one for any thermonuclear plasma whose radius is comparable in size to an alpha particle gyroradius. A proper treatment of the problem would have to allow for the development of space-charge electric fields in a realistic way. This is a problem area which should be given further study, since it is critical for accurately predicting the burn dynamics in a small radius θ-pinch.

D. Filling Pressure.

Assuming 100% particle sweep-up during compression, the plasma density at the ignition point is related to the filling gas pressure p_o (assuming T = 20° C) and the compression ratio by

$$n\ (\text{cm}^{-3}) = \frac{7 \times 10^{13}\ p_o\ (\text{mTorr})}{X_o^2} . \qquad (46)$$

From the above discussion (Model 4), we have, for E_θ = 500 V/cm,

$$X_o = \frac{a}{b} = \frac{0.96}{B^{3/7}\ (\text{kG})} , \qquad (47)$$

and from pressure balance (assuming kT = 5 keV),

$$n_{ig} = 2.48 \times 10^{12}\ B^2\ (\text{kG})\ \text{cm}^{-3}. \qquad (48)$$

Thus the filling pressure is simply related to B by

$$p_o = 3.27 \times 10^{-2}\ B^{8/7}\ (\text{kG})\ \text{mTorr} . \qquad (49)$$

For B = 100, 300, and 500 kG, the required filling pressures are 6.3, 22, and 40 mTorr, which are reasonable values.

E. Coil Volume and Stored Magnetic Energy.

The magnetic field fills the cylindrical coil volume,

$$V = \pi\ b^2\ L , \qquad (50)$$

where b = 2 cm and L is given by Eq. (23).

Substituting, and keeping all lengths in centimeters,

$$V = \frac{2.48 \times 10^{11}}{B^2\ (kG)}\ cm^3\ . \qquad (51)$$

The total stored magnetic energy is

$$E_M = \frac{B^2}{8\pi} \times V(cm^3) \times 10^6\ ergs \qquad (52)$$

for B expressed in kG. Eliminating V between Eqs. (51) and (52) gives, using 10^{13} erg = 1 MJ,

$$E_M = 987\ MJ\ , \qquad (53)$$

independent of the magnetic field strength. This value for E_M is a very modest number, as reactor requirements go. In the RTPR design,[19] for example, the postulated energy storage is about 90 times this value.

F. Energy and Power Output.

The output energy per unit length scales as, from Eq. (8),

$$\frac{E_n}{L} = a^2\ n \times \text{constant}\ . \qquad (54)$$

Since we have n scaling as B^2[Eq. (15)], and a scaling as $B^{-3/7}$ [Eq. (44)], E_n/L scales as

$$\frac{E_n}{L} = B^{8/7} \times \text{constant}. \qquad (55)$$

The total energy output per pulse scales as L x E_n/L, thus

$$E_n = \frac{\text{constant}}{B^{6/7}}\ . \qquad (56)$$

The remarkable fact here is that the energy per pulse decreases as B increases, which is not an intuitive result.

The output power (thermal) scales as

$$P_{TH} = \frac{a^2\ n\ L}{\tau_c} \times \text{constant}, \qquad (57)$$

where the cycle time, τ_c, is assumed to be determined by first-wall loading restrictions. Since $\overline{P}_w/A$ scales as

$$\overline{P}_w/A = \frac{a^2\ n}{b\ \tau_c} \times \text{constant} \qquad (58)$$

and both $\overline{P}_w/A$ and b are constants, by choice, τ_c scales as

$$\tau_c = a^2\ n \times \text{constant}. \qquad (59)$$

Thus the cycle time is simply proportional to E_n/L, the energy per unit length. Substituting Eq. (59) into Eq. (57) gives the scaling law for the total output power:

$$P_{Th} = L \times \text{constant} \qquad (60)$$
$$= \text{constant}/B^2\ .$$

Thus the output power decreases as $1/B^2$, leading to the conclusion that smaller power plants necessitate higher fields.

V. LASER ABSORPTION LENGTH

The basic process for absorption of laser light in a plasma is classical inverse bremsstrahlung.[25] Inverse bremsstrahlung is equivalent to plasma resistance and the formulas can be derived from resistance concepts.[20]

Dawson and collaborators have postulated enhanced absorption when the laser radiation is near the plasma frequency or twice the plasma frequency.[3] The necessary conditions for this mechanism do not prevail in the proposed experiments with CO_2 lasers. It has also been shown theoretically that nonlinear back-scatter processes, i.e., stimulated Raman scattering and stimulated Brillouin scattering, can prevent absorption of the laser light.[26] This phenomenon has not yet been observed experimentally.

We assume here that only classical inverse bremsstrahlung will be operative. The absorption coefficient in this case has been recently updated by Dawson and Johnston:[27]

$$K = 8.66 \times 10^{-30}\ \frac{Z\ n_e^2\ \lambda^2\ \ln \Lambda(\lambda)}{(kT)^{3/2}} \frac{1}{\left(1 - \lambda^2/\lambda_{pe}^2\right)^{1/2}} \qquad (61)$$

where K is in cm^{-1} for n_e in cm^{-3}, λ and λ_{pe} in cm, and kT in eV. The $\Lambda(\lambda)$ term in Eq. (62) is independent of density: $\Lambda(\lambda) = 5.15 \times 10^{-3}\ [kT(eV)]^{3/2}\ \lambda^{-1}$ (cm). For z = 1 and 10.6 μ laser light, the absorption length, $\ell_{ab} = K^{-1}$, is given by

$$\ell_{ab} = 1.03 \times 10^{35} \frac{[kT(eV)]^{3/2}}{n_e^2(cm^{-3})\ \ln \Lambda(\lambda)} \left(1 - \frac{n_e(cm^{-3})}{10^{19}}\right)^{1/2} cm. \tag{62}$$

Eq. (62) is plotted in Figs. 5 and 6. The absorption lengths are agreeably short for temperatures below 1 keV and densities above 10^{17} cm^{-3}, but at a reactor ignition temperature of 5 keV and a density of 4×10^{17} cm^{-3}, the absorption length is approximately 161 m.

Experimental confirmation of Eq. (62) over an interesting regime of parameters is still lacking. Recent measurements[28] of ℓ_{ab} in an argon plasma at 1-2 eV agree with Eq. (62) within about a factor of 2, but suggest a stronger density dependence than n_e^2. We will assume that ℓ_{ab} is correctly given by Eq. (62) in this report.

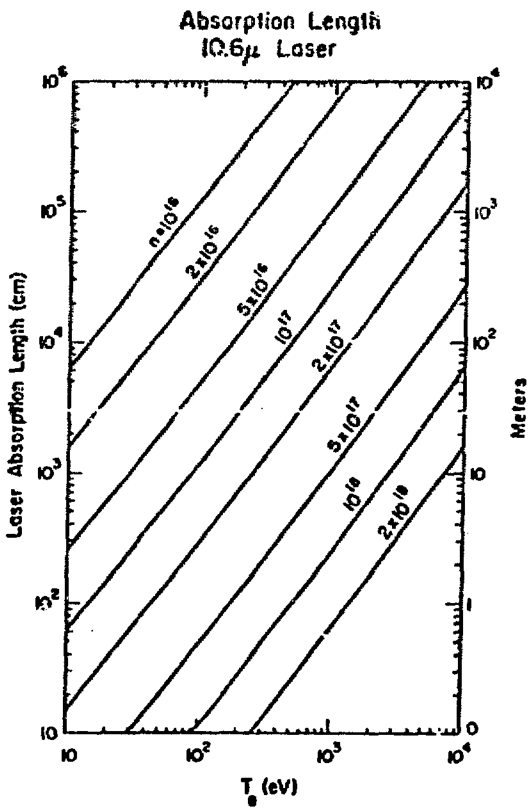

Fig. 5. Absorption length of 10.6 μ light vs electron temperature [Eq. (62)].

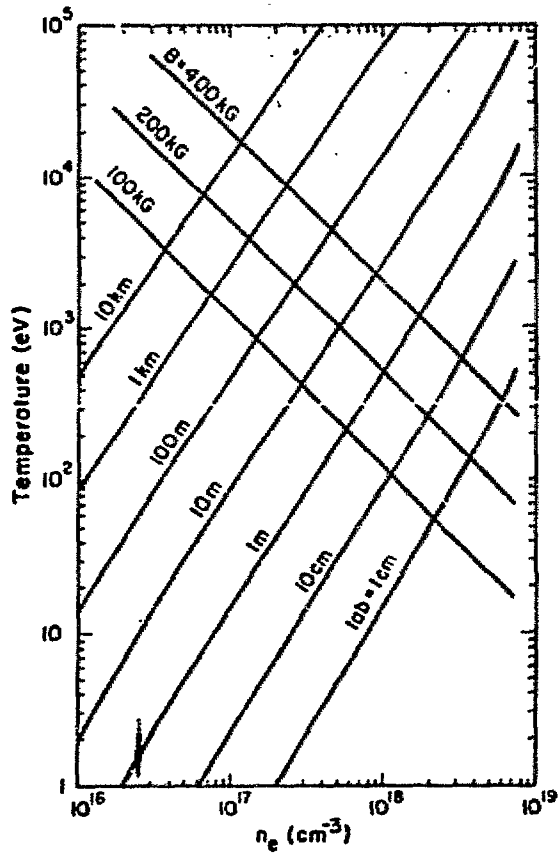

Fig. 6. Absorption length of 10.6 μ light as a function of electron density and temperature [Eq. (62)].

VI. EQUATIONS OF STATE AND MOTION FOR A LASER-HEATED PLASMA COLUMN

A. Introduction.

We consider the problem of a long, dense, initially cold plasma column, confined by an axial magnetic field, which is heated along its length by laser irradiation (inverse bremsstrahlung). We address the question of how the plasma will respond to such heating, assuming that it occurs uniformly along the column length. In particular, we wish to determine whether the plasma accommodates a changing radial pressure balance by altering its beta value, its particle density, or both. This requires that we know how the plasma beta, density, and radius vary as a function of the imposed temperature increase and the initial conditions. Using a sharp boundary MHD model, we find that the plasma tends to increase its beta value first, without significantly increasing its radius, up to $\beta \sim 1/2$. Further increases in temperature increase both beta and radius together until β is nearly unity. Thereafter, the plasma achieves pressure balance entirely by means of radial expansion, further decreasing its density directly as 1/T.

B. The Model.

We take a sharp boundary MHD model for the plasma column, and assume that all properties, including heat addition, are uniform along the length. Explicitly our assumptions are:

1. Charge neutrality ($n_e = n_i = n$)
2. Common temperature for electrons and ions ($T_e = T_i = T$)
3. Constant line density ($N = \pi a^2 n$ = constant)
4. Constant internal flux ($\phi_i = \pi a^2 B_i$ = constant)
5. Constant external field (B_o = constant)
6. Radial pressure balance ($\beta = 1 - (B_i/B_o)^2$)
7. Definition of beta ($2nkT = \beta B_o^2/8\pi$)

C. Solution.

Rewriting the assumptions:

$$na^2 = \text{constant} \tag{63}$$

$$B_i a^2 = \text{constant} \tag{64}$$

$$B_i/\sqrt{1-\beta} = \text{constant} \tag{65}$$

$$\frac{nT}{\beta} = \text{constant} . \tag{66}$$

Substituting Eq. (65) into Eq. (64):

$$a^2\sqrt{1-\beta} = \text{constant} . \tag{67}$$

Substituting Eq. (63) into Eq. (66):

$$\frac{T}{a^2\beta} = \text{constant} . \tag{68}$$

Substituting Eq. (67) into Eq. (68):

$$\frac{\sqrt{1-\beta}}{\beta} T = \text{constant}. \tag{69}$$

Equations (63)-(69) represent conservation laws which must be satisfied as the plasma temperature changes. If the plasma state is characterized at some time by the quantities a_o, β_o, n_o, and T_o, at some later time the plasma properties are a, β, n, and $T > T_o$. The conservation equations (63), (68), and (69) require that:

$$n_o a_o^2 = na^2 \tag{70}$$

$$\frac{T_o}{a_o^2\beta_o} = \frac{T}{a^2\beta} \tag{71}$$

$$\frac{\sqrt{1-\beta_o}}{\beta_o} T_o = \frac{\sqrt{1-\beta}}{\beta} T \tag{72}$$

Equation (72) is quadratic in β/β_o, with solution

$$\frac{\beta}{\beta_o} = \frac{\beta_o}{2(1-\beta_o)} \left(\frac{T}{T_o}\right)^2 \left[\sqrt{1 + \frac{4(1-\beta_o)}{\beta_o^2\,(T/T_o)^2}} - 1\right]. \tag{73}$$

In terms of Eq. (73) the plasma beta, radius and density variations are given by

$$\beta = \frac{\beta_o^2}{2(1-\beta_o)} \left(\frac{T}{T_o}\right)^2 \left[\sqrt{1 + \frac{4(1-\beta_o)}{\beta_o^2\,(T/T_o)^2}} - 1\right] \tag{74}$$

$$\frac{a}{a_o} = \left(\frac{T/T_o}{\beta/\beta_o}\right)^{1/2} \tag{75}$$

$$\frac{n}{n_o} = \left(\frac{1}{a/a_o}\right)^2 \tag{76}$$

as functions of the independent variable T/T_o and initial conditions β_o, a_o, and n_o.

Our model describes both heating and cooling of the plasma column but we will restrict our attention here to the heating case, $T/T_o \geq 1$.

D. Discussion.

Figures 7 and 8 show how the plasma density, beta, and radius change as a function of temperature for two particular initial conditions: (a) $\beta_o = 0.01$ and (b) $\beta_o = 0.20$.

The (a) case, $\beta_o = 0.01$, corresponds (for example) to a plasma of initial density 10^{18} cm^{-3} in a 300 kG field at an initial temperature of 10 eV. The (b) case, $\beta_o = 0.20$, would correspond to the same plasma at a starting temperature of 200 eV. In case (a), the value $T/T_o = 1000$ corresponds to a plasma temperature of 10 keV; in case (b) the 10 keV point is given by $T/T_o = 50$.

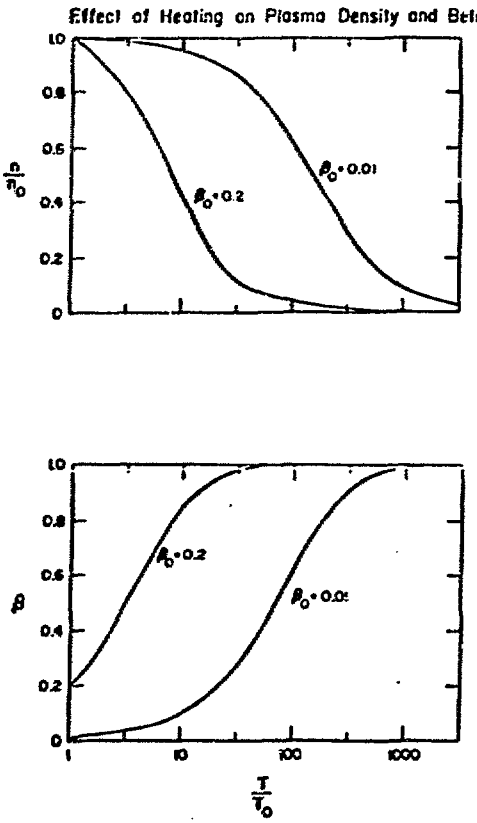

Fig. 7. Effect of uniform axial heating on plasma density and beta.

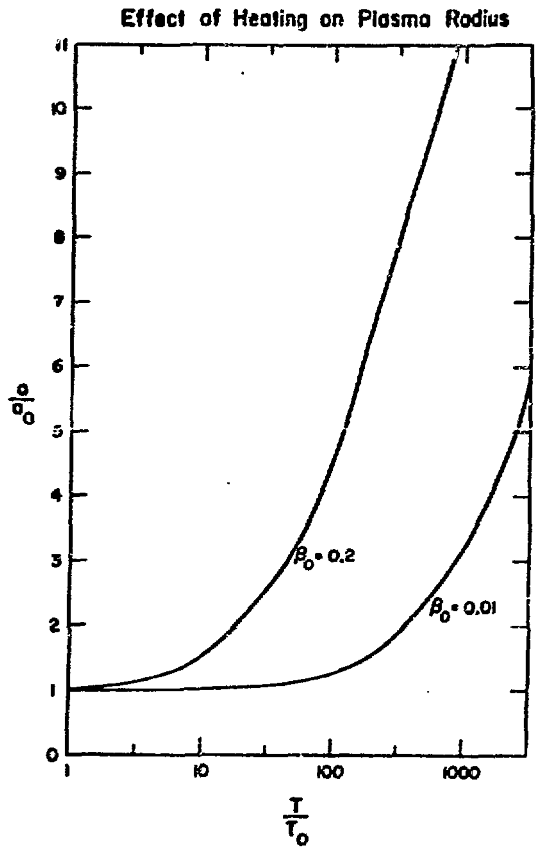

Fig. 8. Effect of uniform axial heating on plasma radius.

Comparing the plasma parameters in cases (a) and (b) at the starting temperature and at the T = 10 keV point, we see that the plasma heating can be divided into three fairly distinct regimes. The first regime occurs when the plasma beta is low. In the low beta regime, heating is manifested almost entirely as a beta increase, with negligible expansion taking place. In case (a), beta increases by roughly a factor of 50, up to $\beta \sim .5$, while the radius increases only 25%. In this phase of the heating, beta increases about linearly with T. In the second regime, beta has a value of a few times 10^{-1}, and heating is accompanied by substantial changes in both beta and radius. In the third regime, the beta curve flattens out near a value of unity, and all heating is accommodated by radial expansion. In this regime, the plasma density is inversely proportional to temperature, $n \propto 1/T$.

E. Conclusions.

A laser-heated plasma column accommodates a heat input which is uniform along its length by increasing both its beta and radius. If beta is initially low, the heating acts to increase beta without appreciably affecting the radius up to beta values of a few tens of percent. Thereafter, beta and radius both increase until beta reaches approximately unity. Further heating is accomplished by a $\beta = 1$ expansion of the plasma with $n \propto \frac{1}{T}$. At a temperature of 10 keV, the column beta is ~ 0.99, irrespective of the starting conditions.

VII. SCALING LAWS FOR A LASER-HEATED REACTOR

In the calculations which follow, we assume that laser-heating of a long plasma column is a technical reality, and we investigate the scaling with B. That is, we assume conditions of classical absorption of the radiation by inverse bremsstrahlung, absence of anomalous back-scatter effects, and a favorable density profile "dipped" in the middle to focus the laser beam initially, if necessary.

The important question of channeling the laser beam along a long narrow column of plasma has been addressed both theoretically [29,30,31] and experimentally,[2] and it is generally accepted that channeling of the laser beam is possible. The back-scatter problem is discussed in Sec. VII-E.

A. Length of a Laser-Heated Reactor.

As in the case of the linear θ-pinch, Sec. IV, we assume that the minimum length of the reactor is governed by end-loss considerations. From Eqs. (23) and (24), the reactor length scales as $1/B^2$ or $1/n$, but until these quantities are specified the reactor length still remains arbitrary.

1. Matching Absorption Length to Reactor Length. The minimum laser energy E_L required is the energy needed to raise the plasma particles to their ignition temperature of 5 keV along the column length. Any excess heating of the input end above 5 keV will, of course, raise the minimum requirement, as will any scattering losses incurred along the column or from the open ends. One can minimize E_L in this respect by matching the reactor length, L, to the laser absorption length, ℓ_{ab}.

Equating L [Eq. (24)] and ℓ_{ab} [Eq. (62)], neglecting the λ/λ_p term, yields

$$\frac{1.03 \times 10^{35}\ (kT)^{3/2}}{n_e^2\ \ell n\Lambda} = \frac{2.4 \times 10^{22}}{\bar{n}} , \qquad (77)$$

where both L and ℓ_{ab} are expressed in cm. Solving for n_e at the ignition point (kT = 5 keV and $(n_e)_{ig} = 2\bar{n}$) and denoting this value of n_e by $(n_e)^*_{ig}$ yields the match condition density as:

$$(n_e)^*_{ig} = 5.28 \times 10^{16}\ cm^{-3}. \qquad (78)$$

In order for the laser beam to be absorbed before exiting the plasma column, the particle density at ignition must satisfy

$$(n_e)_{ig} \geq (n_e)^*_{ig} , \qquad (79)$$

where $(n_e)^*_{ig}$ is given by Eq. (78). This requirement is easily satisfied. For an ignition density of 5.3×10^{16} cm, the average density (assuming $k\bar{T}$ = 10 keV) is $2.6 \times 10^{16}\ cm^{-3}$. This corresponds to a magnetic field of 146 kG, from Eq. (1), and a minimum reactor length of 9.24 km. Furthermore, to avoid the possibilities of alpha particle collisions with the wall the magnetic field should exceed 137 kG for a 2 cm radius coil (Sec. IV-C). Thus the laser absorption requirements are automatically met in a fusion reactor operating in the 150 kG range or above.

2. Selection of Magnetic Field. For a design point, we choose B = 400 kG. The scaling laws of Sec. IV then yield the following reactor parameters: average density during burn $\bar{n} = 2 \times 10^{17}\ cm^{-3}$, density at ignition (5 keV) $(n_e)_{ig} = 4 \times 10^{17}\ cm^{-3}$, reactor length L = 1200 n, and burn time τ_B = 5 msec. The laser absorption length at ignition is ℓ_{ab} = 161 m.

B. Laser Energy Requirements.

The laser energy requirements may be treated in two parts: (1) the energy required to heat the plasma to 5 keV (intrinsic energy requirement) and (2) energy wasted in unavoidable losses or excess local heating above 5 keV.

1. Plasma Energy Content. The kinetic energy density associated with a Maxwellian plasma is $nk(T_e + T_i)$, and for a β = 1 plasma this will equal the magnetic energy density excluded, $B^2/8\pi$. Thus the total energy in the plasma column may be written

$$E_p = \frac{B^2}{8\pi} \times \pi\ a^2 \times L, \qquad (80)$$

where a is the plasma radius and L is the column length. In more convenient units

$$E_p(J) = 1.25\ B^2\ (kG)\ a^2\ (cm)\ L\ (m)\ . \qquad (81)$$

Eq. (81) is plotted in Fig. 9 as E_p/L in J/meter.

Substituting Eq. (23) for the end-loss length,

$$L = \frac{1.97 \times 10^8}{B^2\ (kG)}\ \text{meters} \qquad (23)$$

into Eq. (81) and identifying E_p as the intrinsic laser energy yields

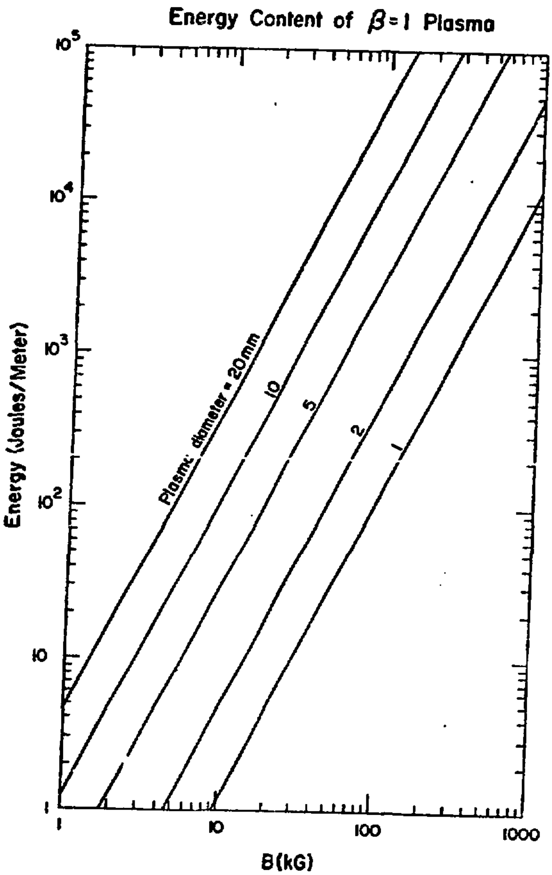

Fig. 9. Energy content of a $\beta = 1$ plasma column as a function of magnetic field strength and plasma diameter.

$$E_L(J) = 2.46 \times 10^8\ a^2\ (cm). \tag{82}$$

We note that the laser energy in Eq. (82) is <u>independent</u> of B, of n, and of L. E_L depends only on the plasma cross-sectional area, and minimizing the plasma radius a will therefore minimize the size of the laser required.

<u>a. Plasma Radius.</u> The minimum plasma radius quoted for the laser-heated reactor varies greatly, depending on the source.[1-3] The absolute minimum is set by an ion gyroradius. Thus, from Eq. (30):

$$r_B(T) = \frac{16.2}{B(kG)}\ cm\ , \tag{83}$$

where $r_B(T)$ is the triton gyroradius at 5 keV. For B = 400 kG, $r_B(T)$ is 0.41 mm.

Humphries[29,30] has calculated mode structures for a multiple-pass laser heating system using $\lambda = 10.6\ \mu$, and has found beam widths of 1-3 mm.

Dawson[3] has estimated the minimum radius at 1-2 cm, the exact value depending on the rate of radial diffusion and conduction losses.

The alpha particle gyroradius may set a lower limit on the plasma column size of 1-2 cm, at some stage in the burn, as discussed in Sec. IV. C. It is not yet clear to what extent this restriction will conflict with the assumption of a much smaller plasma column (1-2 mm) during the ignition phase.

For a = 1 cm, Eq. (82) requires a laser energy of ∿ 250 MJ; for a = 1 mm, the requirement is ∿ 2.5 MJ. 2.5 MJ is roughly two orders of magnitude above presently available N_2-CO_2 laser systems operated in the long-pulse mode.[32]

<u>2. Unavoidable Light Losses.</u> For a 400 kG field, the ratio of reactor length to absorption length is $L/\ell_{ab} = 8.6$. In this situation, there should be negligible light loss out of the open ends of the plasma column, and the losses incurred will be due primarily to overheating at the input end.

<u>a. The Plasma as a Light Pipe.</u> In order for the laser beam to be used efficiently, the laser light must be able to propagate from the hot regions of the column to the cold, unheated regions without a great deal of "over-heating" in the hot regions. That is, the plasma must rapidly become transparent to the laser beam above 5 keV. Otherwise, the laser energy requirements will become prohibitive. It is also unfortunately true that as the plasma becomes transparent, it may lose its ability to focus the laser beam along the field lines. Thus side-scatter, or possibly even complete loss of the beam, may become a problem.

<u>b. Plasma Transparency vs Temperature.</u> Two factors work to make the plasma become transparent quite rapidly above 5 keV. The first of these is the explicit increase of the absorption length with temperature, as given by Eq. (62). For densities less than ∿ 10^{18} cm^{-3}, ℓ_{ab} is given by

$$\ell_{ab}\ (cm) = \frac{1.03 \times 10^{35} [kT(eV)]^{3/2}}{n_e^2\ (cm^{-3})\ \ell n\ \Lambda}\ . \tag{84}$$

The second factor is the decrease in density, which is also a consequence of higher temperatures. From the equation-of-state study in Sec. VI, we found that the plasma beta is approximately unity at ignition, irrespective of the detailed starting conditions. In this regime the plasma responds to heating by a $\beta = 1$ expansion, i.e., $n \propto 1/T$. The exact relationship is, from Eq. (1),

$$n\ (\mathrm{cm}^{-3}) = \frac{1.24 \times 10^{13}\ B^2\ (\mathrm{kG})}{kT\ (\mathrm{eV})} . \qquad (85)$$

Substituting n from Eq. (85) into Eq. (84) yields

$$\ell_{ab}\ (\mathrm{cm}) = \frac{2.12 \times 10^{13}\ [kT(\mathrm{keV})]^{7/2}}{\ell n\ \{1.54 \times 10^5\ [kT(\mathrm{keV})]^{3/2}\}} \frac{1}{B^4(\mathrm{kG})} \qquad (86)$$

for kT in keV. In the case where B = 400 kG,

$$\ell_{ab}(\mathrm{cm}) = \frac{8.28 \times 10^2\ [kT(\mathrm{keV})]^{7/2}}{\ell n\ \{1.54 \times 10^5\ [kT(\mathrm{keV})]^{3/2}\}} . \qquad (87)$$

Thus ℓ_{ab} is a strong function of temperature. An increase in kT from 5 keV to 10 keV would increase ℓ_{ab} by a factor of 10.6, from 161 m to 1700 m, which is greater than the length of the reactor. To put it another way, if we require that the temperature everywhere along the plasma column be raised to $\geq$ 5 keV, then about 80% or so of the column must be heated to around 10 keV in order to achieve the necessary transparency to ignite the final 20% of plasma.

3. Summary of Losses. The intrinsic laser energy requirements can be kept to about 2.5 MJ by restricting a to 1 mm. Neglecting losses from the ends, the remaining energy losses are due to plasma transparency requirements, which lead to overheating. We find these losses to be approximately 100% of the intrinsic energy requirements. Taken together, these lead to a minimum laser energy of ~ 5 MJ.

It may be desirable to heat the plasma column from both ends, utilizing a dual laser system. The laser development problem can be alleviated considerably by "stacking" a number of smaller lasers and combining the beams at a common focus.

C. Laser Power Requirements.

For a repetitively pulsed reactor with cycle time τ_c, the input power required by the laser is

$$P_L = \frac{E_L}{\tau_c \eta_L} \text{ watts,} \qquad (88)$$

where η_L is the electrical-energy-to-light efficiency of the laser, and E_L is the laser energy output in joules. If the laser is used to heat a fusion reactor plasma to ignition, then the fact that one must obtain more useful fusion energy than is required by the laser (by at least a factor of 10 if the reactor is to be interesting) puts a high premium on laser efficiency.

The CO_2-N_2 laser system is fortunately a good performer in this respect, especially in the slow-pulse (μsec time scale) mode. For example, if E_L = 5 MJ and τ_c = 0.5 sec, then the presently obtainable value of η_L, about 30%, leads to a laser input power (pump) requirement of approximately 30 MW.

D. Magnetic Energy Storage Requirements.

The minimum magnetic energy storage requirement is set by the choice of coil bore, as discussed in Sec. IV:

$$E_M = 2.46 \times 10^2\ b^2\ (\mathrm{cm})\ \ \mathrm{MJ} . \qquad (89)$$

Since there is no magnetic compression in the laser system, it would seem that the coil could have a much smaller diameter than its theta-pinch counterpart, and other authors have pointed this out.[3] However, the alpha particles, with a birth energy of 3.52 MeV, can collide with the wall unless their gyroradius

$$r_B\ (\alpha) = \frac{272}{B(\mathrm{kG})}\ \mathrm{cm} \qquad (90)$$

does not exceed b. At 400 kG, the alpha gyroradius is 0.7 cm. Thus the coil radius b must be at least this large, plus the plasma radius (0.1 cm). For b = 1.0 cm, the magnetic storage requirement, from Eq. (89), is ~ 250 MJ. This, we note, is some 50 times the required laser energy.

E. The Backscatter Problem.

An example will illustrate the backscatter problem. Consider a reactor operating with a 400 kG field: the reactor length is ~ 1200 meters, the ion density is $2 \times 10^{17}\ \mathrm{cm}^{-3}$, and the burn time is ~ 5 milliseconds. If the laser supplies its energy in a 500 μs pulse, then the "risetime" for heating is 500 μs, or about 1/10 of the burn time; if the laser pulse is 50 μs long, then the heating time is about 1% of the burn time. The beam power of the laser in these two cases will be 10^{10} watts or 10^{11} watts, respectively, for E_L = 5 MJ. The beam power density will therefore be 3×10^{11} or 3×10^{12} watts/cm^2, respectively, for a = 1 mm, which is above the theoretically predicted threshold for large anomalous backscatter.

A possible way around this dilemma is to use the laser beam to heat the plasma prior to adiabatic compression in a rising magnetic field. In this scheme the laser replaces shock-heating as the preheat stage, which would benefit the θ-pinch by removing this component outside the reactor. It would also benefit the laser by greatly reducing the energy requirements, since the plasma would now be heated to ignition by magnetic compression. Backscatter is theoretically reduced because the laser energy is down (by about an order of magnitude) and the cross-sectional area of the beam is increased (by roughly a factor of $(1\ \mathrm{cm}/0.1\ \mathrm{cm})^2 = 100$). Thus the beam power density is reduced approximately three orders of magnitude. There are difficulties involving the laser penetration distance, however, and we will not dwell on this problem any further, as there is as yet no experimental verification of the backscatter predictions.

VIII. *REACTOR PARAMETERS AT 400 kG*

Once the magnetic field has been specified, the other reactor parameters follow immediately, because B has been kept as the independent variable in the equations. The two reactor models require different-sized coil bores because compressional heating is not required in the laser-heated reactor case. Otherwise, they are generally similar.

A. Theta-Pinch Reactor.

For B = 400 kG, and an assumed plasma temperature $k\overline{T}$ = 10 keV and $\overline{n}\tau = 10^{15}$ cm^{-3} sec, we have: $\overline{n} = 2 \times 10^{17}$ cm^{-3}, b = 2.0 cm, a = 0.15 cm, L = 1.2 km, E_M = 987 MJ, and τ_B = 5 msec.

From the scaling law discussion in Sec. III,

$$E_n/L = 3.22 \times 10^{-5}\ a^2\ B^2 \quad \mathrm{MJ/m}\ , \tag{91}$$

for a in cm and B in kG. Substituting,

$$E_n/L = 0.116 \quad \mathrm{MJ/m}\ . \tag{92}$$

For a reactor length of 1.2 km,

$$E_n = 139\ \mathrm{MJ}\ . \tag{93}$$

The cycle time is determined by the permissible wall loading, $\overline{P}_w/A$. From Eq. (13b),

$$\tau_c = 3.80 \times 10^{-4}\ \frac{a^2\ B^2}{b}\ \frac{1}{\overline{P}_w/A}\ , \tag{94}$$

where τ_c is in seconds for $\overline{P}_w/A$ in MW/m^2. An upper limit for $\overline{P}_w/A$ is probably 3.5 MW/m^2.[4] Choosing a more conservative value of 2.0 MW/m^2 yields

$$\tau_c = 0.34\ \mathrm{sec.} \tag{95}$$

With this choice of cycle time, the thermal power is calculated from Eq. (2):

$$P_{Th} = E_n/\tau_c \tag{96}$$
$$= 409\ \mathrm{MW}\ .$$

The electrical output from the plant is related to P_{Th} by

$$P_{elec} = \eta\ P_{Th}\ , \tag{97}$$

where η is the overall thermal conversion efficiency of the plant. Assuming η = 0.50 yields

$$P_{elec} = 205\ \mathrm{MWe}\ . \tag{98}$$

This is a relatively small output for a fusion reactor (RTPR, for example, has an output of several GW), which is advantageous from the point of view of capital costs, siting, small users, etc.

A useful figure of merit for measuring how efficiently magnetic field is utilized in a fusion reactor is given by

$$\tau_m = \frac{E_M}{P_{elec}}\ , \tag{99}$$

i.e., the ratio of stored magnetic energy to plant electrical output. Substituting, we find

$$\tau_m = 4.8\ \mathrm{sec.}$$

That is, the reactor running at full power would completely charge the magnetic energy storage system in 4.8 seconds.

B. Laser-Heated Reactor.

For B = 400 kG, $k\bar{T}$ = 10 keV, and $\bar{n}\tau = 10^{15}$ cm^{-3} sec, we find: $\bar{n} = 2 \times 10^{17}$ cm^{-3}, b = 1.0 cm, a = 0.10 cm, L = 1.2 km, E_M = 250 MJ, and τ_B = 5 msec.

Following the same procedure used in Sec. VIII-A above, we have evaluated E_n/L, E_n, τ_c, P_{Th}, P_{elec}, and τ_m for the laser-heated reactor case. The results are given in Table I.

TABLE I

REACTOR PARAMETERS AT 400 kG

Quantity	Symbol	Units	θ-Pinch Reactor	Laser-Heated Reactor
Lawson parameter	$\bar{n}\tau_B$	cm^{-3} sec	10^{15}	10^{15}
Magnetic field	B	kG	400	400
Average temperature	$k\bar{T}$	keV	10	10
Average ion density	$\bar{n}$	cm^{-3}	2×10^{17}	2×10^{17}
Plasma radius	a	cm	0.15	0.10
Coil radius	b	cm	2.0	1.0
Reactor length	L	km	1.2	1.2
Burn time	τ_B	msec	5	5
Energy per unit length	E_n/L	MJ/m	0.12	0.05
Total energy	E_n	MJ	140	62
Cycle time	τ_c	sec	0.34	0.30
Thermal power	P_{Th}	MW	409	207
Electrical power	P_{elec}	MWe	205	103
Quality factor	τ_M	sec	4.8	2.4
Magnetic energy storage	E_M	MJ	987	246

C. Summary and Conclusions.

We have attempted to provide a basis for comparing the magnetically heated θ-pinch reactor and its laser-heated counterpart, using the same ground rules for both. We have not attempted to do a detailed energy balance in either case, since that would require specific models for reactor components which are not yet designed. In the spirit of fairness, we have given both models equal neglect in this regard.

Some differences between the two reactor models are apparent in Table I. The laser-heated reactor would appear to have some advantages, relatively minor, over the theta pinch, namely: a smaller plant size (by a factor of 2), a smaller amount of stored magnetic energy (by a factor of 4), a smaller bore - and hence, presumably, less difficulty in reaching 400 kG without damaging the coil - (by a factor of 2), and more efficient use of its magnetic field, as measured by the τ_M parameter (by a factor of 2). These advantages all accrue from the smaller coil bore, which is made possible by eliminating compressional heating. Against these advantages must be set the difficulty of procuring at least 5 MJ of laser light, 3 times a second (a laser input energy of ∿ 50 MW), and the largely unknown physics problems involved in heating a plasma filament over 1000 meters long to a temperature of 5 keV by means of photon absorption from the ends.

The linear θ-pinch, on the other hand, involves more familiar technology, and, if 400 kG is indeed feasible, then this geometry offers some attractive advantages over toroidal reactor designs. As compared to the current RTPR design,[19] the linear θ-pinch reactor discussed above requires about 80 times less magnetic energy storage, 1/10 the minimum plant size, and a more efficient utilization of magnetic field, based on the τ_M parameter, of about a factor of 15.

We conclude that the high field reactor concept is worthy of further study. The laser method of heating provides a possible alternative to conventional magnetic heating, but it is presently unknown whether the laser method will work, and if so, whether 5 MJ lasers will become available.

A hybrid system involving some combination of laser and magnetic heating is also a possibility which should be explored.

ACKNOWLEDGMENTS

We wish to acknowledge the valuable contributions of J. P. Freidberg and F. L. Ribe as well as several helpful discussions with G. Vlases of the University of Washington.

REFERENCES

1. A. Hertzberg, AIAA paper 73-258, presented at AIAA 11th Aerospace Sciences Meeting, Washington Jan. 1973.

2. N. A. Amherd and G. C. Vlases, Proceedings 2nd Topical Conference on Pulsed, High-β Plasmas, Garching, July 1972. Garching Laboratory Report IPP 1/127, 1972, p. 241. Also, G. C. Vlases, Proc. Japan-U.S. Seminar on Laser Interactions with Matter, Sept. 1972.

3. J. M. Dawson, A. Hertzberg, R. E. Kidder, G. C. Vlases, H. G. Ahlstrom, L. C. Steinhauer, Plasma Physics and Controlled Nuclear Fusion Research, (IAEA, Vienna, 1971) Vol. I, p. 673.

4. S. C. Burnett, W. R. Ellis, T. A. Oliphant, and F. L. Ribe, Los Alamos Scientific Laboratory Report LA-5121-MS (1972).

5. H. Knoepfel, Pulsed High Magnetic Fields, (North Holland Publishing Co., Amsterdam, 1970).

6. A. Bailey, G. Boicourt, K. Hanks, Los Alamos Scientific Laboratory Report, LA-5250-PR (1973). Also unpublished P-16 quarterly report, May 1972.

7. W. H. Bergmann, Proceedings of the International Symposium on Magnet Technology, Stanford, California, 1965. USAEC Report CONF-650922.

8. S. Foner and W. G. Fisher, Rev. Sci. Inst. 38, 440 (1967).

9. H. Knoepfel and R. Lupi, Journal of Physics E: Scientific Instruments 5, 1133 (1972).

10. S. Chikazumi, S. Tanuma, I. Oguro, F. Ono, and K. Tajima, IEEE, Transactions on Magnetics, Vol. Mag. 5, No. 3, Sept. 1969.

11. S. Foner and H. H. Kolm, Rev. Sci. Inst. 28, 799 (1957).

12. R. A. Smith, Physics Education (GB), 4, 326 (1970).

13. A. M. Andrianov, V. F. Demichev, G. A. Eliseev, P. A. Levit, I. V. Kurchatov Institute Report IAE-2025, 1970.

14. C. M. Fowler, Science 180, 261 (1973).

15. R. J. Weggel and D. B. Montgomery, Proceedings Fourth International Conference on Magnet Technology, Brookhaven, 1972. U.S.A.E.C. Report CONF - 720908, p. 18.

16. B. E. Mulhall, Proceedings Fourth International Conference on Magnet Technology, Brookhaven, 1972. U.S.A.E.C. Report, CONF-720908, p.360.

17. J. C. Vallier, Proceedings Fourth International Conference on Magnet Technology, Brookhaven, 1972. U.S.A.E.C. Report, CONF-720908, p. 233.

18. S. Foner, E. J. McNeff, Jr., B. T. Matthias, T. H. Geballe, R. H. Willens, and E. Corenzwit, Physics Letters 31A, 349 (1970).

19. W. R. Ellis, R. A. Krakowski, T. A. Oliphant, Jr., and F. L. Ribe, "The Status of the RTPR Engineering Design: An Update," Los Alamos Scientific Laboratory Report LA-UR-73-515, (1973).

20. J. P. Freidberg, private communication.

21. J. B. Taylor and J. A. Wesson, Nuclear Fusion 5, 159 (1965).

22. K. S. Thomas et al., "Plasma Experiments on the Linear Scyllac Theta Pinch," submitted to the Physics of Fluids for publication, October, 1973.

23. See for example R. Z. Sagdeev, Rev. Plasma Physics, edited by M. A. Leontivich, Consultants Bureau (1966).

24. F. L. Ribe, et al., Los Alamos Scientific Laboratory Report LA-5026-P (1973).

25. L. Spitzer, Jr., Physics of Fully Ionized Gases, (Interscience Publishers, New York, 1956), p. 89.

26. D. W. Forslund, J. M. Kindel, and E. L. Lindman, Phys. Rev. Letters 30, 739 (1973).

27. T. W. Johnston and J. M. Dawson, Phys. Fluids 16, 722 (1973).

28. M. F. Weisback and H. G. Ahlstrom, Phys. Fluids 16, 1164 (1973).

29. S. Humphries, Multiple-Pass Laser Heating of a Magnetically Confined Plasma, Los Alamos Scientific Laboratory Report LA-5010, (1972).

30. S. Humphries, Multipass Systems for CO_2 Laser Heating and Diagnostic Scattering Experiments, Los Alamos Scientific Laboratory Report LA-5167-MS, (1973).

31. L. C. Steinhauer and G. C. Vlases, Phys. Fluids 14, 1109 (1971).

32. T. A. Stratton, private communication.

JD:344(120)